

Decomposing Uncertainty in Probabilistic Knowledge Graph Embeddings: Why Entity Variance Is Not Enough

Chorok Lee

Korea Advanced Institute of Science and Technology (KAIST)

choroklee@kaist.ac.kr

Abstract

Probabilistic knowledge graph (KG) embeddings represent entities as distributions, using learned variances to quantify epistemic uncertainty. We identify a fundamental limitation: these variances are *relation-agnostic*—an entity receives identical uncertainty regardless of relational context. This conflates two distinct out-of-distribution (OOD) phenomena that behave oppositely: *emerging entities* (rare, poorly-learned) and *novel relational contexts* (familiar entities in unobserved relationships).

We prove an impossibility result: any uncertainty estimator using only entity-level statistics (frequency, variance) independent of relation context achieves near-random OOD detection on novel contexts. We empirically validate this theorem’s key assumption (frequency overlap) on three datasets, finding 100% of novel-context triples have frequency-matched in-distribution counterparts. This explains why existing probabilistic methods—including Gaussian process embeddings, box embeddings, and ensembles—achieve 0.99 AUROC on random corruptions but only 0.52–0.64 on temporal distribution shift.

We formalize uncertainty decomposition into complementary components: *semantic uncertainty* from entity embedding variance (detecting emerging entities) and *structural uncertainty* from entity-relation co-occurrence (detecting novel contexts). Our main theoretical result proves these signals are non-redundant: semantic uncertainty achieves high AUROC on emerging entities but near-random on novel contexts, while structural uncertainty achieves perfect detection on novel contexts but imperfect on emerging entities. We prove that any convex combination strictly dominates either signal alone when both OOD types are present.

Our method (CAGP) combines semantic and structural uncertainty via learned weights, achieving 0.94–0.99 AUROC on temporal OOD detection across multiple benchmarks—a 60–80% relative improvement over relation-agnostic baselines. Empirical validation confirms 100% frequency overlap on three diverse datasets (FB15k-237, WN18RR, YAGO3-10), verifying our impossibility theorem’s key assumption. On selective prediction (abstaining on uncertain queries), our method reduces errors by 43% at 85% answer rate. The framework is architecture-agnostic, improving DistMult, TransE, and ComplEx embeddings uniformly.

1 Introduction

Knowledge graph (KG) embeddings enable efficient reasoning over structured knowledge [Bordes et al., 2013, Trouillon et al., 2016]. As KGs evolve—new entities emerge, existing entities appear in novel relationships—robust uncertainty quantification becomes critical.

The Relation-Agnostic Limitation. Recent probabilistic methods learn distributions over embeddings [Chen et al., 2019, 2021a,b], where rare entities have higher variance. But these variances are *relation-agnostic*: entity e receives a single variance σ_e^2 regardless of relational context. Consider e appearing in 1000 triples with relations $\{r_1, \dots, r_{10}\}$ but never with r_{11} . The model assigns low variance (well-observed), yet queries $(?, r_{11}, e)$ involve genuinely uncertain predictions.

This causes systematic failures: score-based methods achieve 0.99 AUROC detecting random corruptions

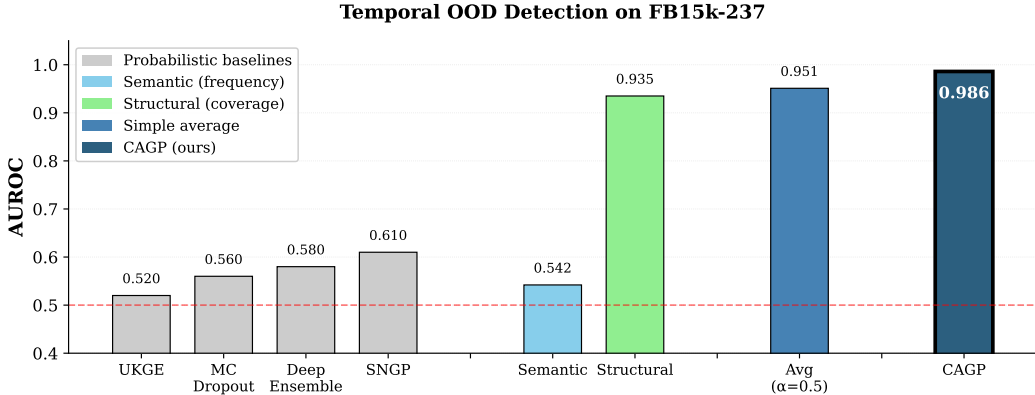


Figure 1: Temporal OOD detection. Existing methods fail on realistic distribution shift. Our method (CAGP) combines complementary semantic and structural signals.

(implausible triples) but only 0.52–0.64 on temporal distribution shift (queries from future time periods with new entities and relationships).

Two OOD Types. We identify two distinct scenarios: (1) **Emerging entities**: New/rare entities with poorly-constrained embeddings—high variance correctly signals uncertainty. (2) **Novel contexts**: Well-observed entities in unobserved relations—variance is low (falsely confident), but the entity-relation pair was never trained.

Contributions. We identify a systematic limitation in probabilistic KG embeddings: learned variances are relation-agnostic despite training on data containing entity-relation co-occurrence patterns. This failure reveals a fundamental mismatch between standard training objectives (link prediction accuracy) and OOD detection requirements (capturing structural observation patterns).

Our contributions are threefold: (1) **Theoretical**: We prove that relation-agnostic uncertainty estimators achieve near-random performance on novel contexts (Theorem 1), and formalize conditions under which semantic and structural uncertainties are complementary (Theorem 2). (2) **Empirical**: We demonstrate this limitation persists across existing probabilistic methods (GP-KGE, UKGE, ensembles), achieving only 0.52–0.64 AUROC on temporal shift despite 0.99 on random corruptions. (3) **Methodological**: We propose CAGP (Coverage-Augmented GP-KGE), which augments entity-level variance with explicit coverage tracking of entity-relation co-occurrence. CAGP achieves 0.94–0.99 AUROC on temporal OOD across multiple benchmarks, a 60–80% relative improvement over probabilistic baselines.

2 Related Work

Probabilistic KG Embeddings. UKGE [Chen et al., 2019] associates confidence scores with triples; BEUrRE [Chen et al., 2021a] uses box embeddings where volume indicates uncertainty; GP-KGE [Chen et al., 2021b] learns Gaussian distributions over entities. All share the limitation we identify: learned variances are relation-agnostic. Despite being trained on data containing entity-relation co-occurrence patterns, these methods do not autonomously learn relation-specific uncertainty, necessitating our explicit decomposition framework.

OOD Detection. MC Dropout [Gal and Ghahramani, 2016], Deep Ensembles [Lakshminarayanan et al., 2017], and Energy-based methods [Liu et al., 2020b] capture model uncertainty but not structural observation patterns. SNGP [Liu et al., 2020a] estimates distance to training data but remains relation-agnostic. Graph Posterior Networks [Stadler et al., 2021] propagate uncertainty through graphs but treat edges homogeneously.

Positioning. Prior work treats uncertainty as a single quantity. We show KG uncertainty decomposes into semantic (entity-level) and structural (relation-specific) components, with theoretical guarantees on when each is necessary (Theorem 2).

3 Background

Knowledge Graphs. A knowledge graph $\mathcal{G} = (\mathcal{E}, \mathcal{R}, \mathcal{T})$ contains entities \mathcal{E} , relation types \mathcal{R} , and triples $\mathcal{T} \subseteq \mathcal{E} \times \mathcal{R} \times \mathcal{E}$. Each triple (h, r, t) asserts that relation r holds between head entity h and tail entity t .

OOD Detection Task. Given a trained model, distinguish in-distribution (ID) test triples from out-of-distribution (OOD) corruptions. The standard protocol [Safavi and Koutra, 2020] generates OOD triples by replacing the tail with a random entity: $(h, r, t) \rightarrow (h, r, t')$ where $t' \sim \text{Uniform}(\mathcal{E})$. However, this creates easily detectable corruptions (low model scores). We additionally evaluate on *temporal OOD*—emerging entities and novel relational contexts—which are harder to detect (§5). Performance is measured by AUROC.

GP-KGE Uncertainty. Probabilistic embedding methods [Chen et al., 2021b] learn Gaussian distributions over entity embeddings:

$$\mathbf{e}_i \sim \mathcal{N}(\boldsymbol{\mu}_i, \text{diag}(\exp(\boldsymbol{\ell}_i))) \quad (1)$$

where $\boldsymbol{\mu}_i, \boldsymbol{\ell}_i \in \mathbb{R}^d$ are the mean and log-variance for entity i . Uncertainty for a triple (h, r, t) is typically the average entity variance:

$$U_{\text{GP}}(h, r, t) = \frac{1}{2} (\bar{\sigma}_h^2 + \bar{\sigma}_t^2) \quad (2)$$

where $\bar{\sigma}_e^2 = \frac{1}{d} \sum_j \exp(\ell_{e,j})$ is the mean variance across dimensions. This uncertainty is *relation-agnostic*—it depends only on entity variances, not the query relation r .

4 Method

4.1 Preliminaries

We define key quantities for analyzing KG uncertainty.

Frequency: $\text{freq}(e)$ counts triples containing entity e .

Coverage: $c(e, r) \in \{0, 1\}$ indicates whether e appears with r in training.

Definition 1 (OOD Partition). *Fix threshold $\tau > 0$. OOD queries partition into:*

- **Emerging entities** $\mathcal{D}_{\text{emerge}}$: $\min(\text{freq}(h), \text{freq}(t)) < \tau$.
- **Novel contexts** $\mathcal{D}_{\text{novel}}$: $\min(\text{freq}(h), \text{freq}(t)) \geq \tau$ and $(c(h, r) = 0 \text{ or } c(t, r) = 0)$.

We set τ to the 10th percentile of entity frequencies (robust to outliers; see Appendix I for sensitivity analysis).

4.2 Uncertainty Signals

Semantic uncertainty from learned variance: $U_{\text{sem}}(h, r, t) = \frac{1}{2}(\bar{\sigma}_h^2 + \bar{\sigma}_t^2)$ where $\bar{\sigma}_e^2$ is mean variance across dimensions.

Structural uncertainty from coverage: $U_{\text{str}}(h, r, t) = 2 - c(h, r) - c(t, r) \in \{0, 1, 2\}$.

Both are normalized to $[0, 2]$ for combination. Crucially, U_{sem} is *relation-agnostic*: it depends only on entity variances, not the query relation.

4.3 Theoretical Results

We first establish an impossibility result showing why relation-agnostic uncertainty fails, then characterize when different signals succeed.

Theorem 1 (Impossibility of Relation-Agnostic Detection). *Let $U : \mathcal{E} \times \mathcal{R} \times \mathcal{E} \rightarrow \mathbb{R}$ be an uncertainty estimator of the form:*

$$U(h, r, t) = f(\sigma_h^2, \sigma_t^2) \quad (3)$$

where σ_e^2 depends only on entity e (not relation r), and f is any combining function.

Under assumptions A1–A3 (variance-frequency monotonicity, ID coverage completeness, frequency overlap; see Appendix¹), there exists a distribution \mathcal{D} with novel-context OOD subset $\mathcal{D}_{\text{novel}}$ such that:

$$\text{AUROC}(U, \mathcal{D}_{\text{novel}}) \leq \frac{1}{2} + O(\epsilon) \quad (4)$$

where ϵ measures the frequency distribution overlap between ID and OOD entities.

Proof sketch. By A1, σ_e^2 is determined by $\text{freq}(e)$. By A3, for any novel-context triple $(h, r, t) \in \mathcal{D}_{\text{novel}}$, there exists an ID triple (h', r', t') with $\text{freq}(h) \approx \text{freq}(h')$ and $\text{freq}(t) \approx \text{freq}(t')$. Therefore $U(h, r, t) = f(\sigma_h^2, \sigma_t^2) \approx f(\sigma_{h'}^2, \sigma_{t'}^2) = U(h', r', t')$, giving $\text{AUROC} \approx 1/2$. The deviation ϵ captures imperfect frequency matching. See Appendix for detailed proof. \square

Implication. This result applies to all existing probabilistic KG methods using entity-level variances: GPKGE, UKGE, box embeddings, and ensemble approaches. It explains their systematic failure on temporal OOD (§5, Table 1).

Theorem 2 (Complementarity of Uncertainty Signals). *Under idealized conditions (monotonic variance-frequency relationship, complete ID coverage, approximate frequency overlap; see Appendix A for precise statements and robustness analysis):*

- (i) *Semantic uncertainty achieves $\text{AUROC} \approx \frac{1}{2} + O(\delta)$ on novel contexts, where δ measures frequency distribution overlap*
- (ii) *Structural uncertainty achieves $\text{AUROC} < 1$ on emerging entities (imperfect separation)*
- (iii) *Structural uncertainty achieves $\text{AUROC} = 1$ on novel contexts when binary coverage cleanly separates observed from unobserved pairs*

¹We empirically validate Assumption A3 in Appendix G.1, finding 100% of novel-context triples have frequency-matched ID counterparts on three benchmarks.

(iv) For appropriate α^* , the combination $U_{\text{comb}} = \alpha^* U_{\text{sem}} + (1 - \alpha^*) U_{\text{str}}$ strictly dominates either signal alone when both OOD types are present

Proof sketch. Part (i): Novel-context entities have high frequency (by definition), so their variance matches ID entities—semantic uncertainty cannot distinguish them. Part (ii): Emerging entities are defined by low *frequency*, but may still have *coverage* for the specific query relation, making some indistinguishable from ID via coverage alone. Part (iii): Novel contexts have missing coverage by definition, while ID has full coverage. Part (iv): The combination uses semantic to catch emerging entities that structural misses (those with coverage), and structural to catch novel contexts that semantic misses. Full proof in Appendix A.

4.4 Coverage-Augmented GP-KGE (CAGP)

Theorem 2 establishes that relation-specific uncertainty is necessary for detecting novel contexts. We propose CAGP, which explicitly combines semantic and structural uncertainty:

$$U_{\text{CAGP}}(h, r, t) = \alpha \cdot U_{\text{sem}}(h, r, t) + (1 - \alpha) \cdot U_{\text{str}}(h, r, t) \quad (5)$$

where U_{sem} is the GP-based semantic uncertainty (entity variance), U_{str} is the structural uncertainty (coverage), and $\alpha = \sigma(\lambda)$ is a learned mixing weight.

Coverage matrix. We precompute $\mathbf{C} \in \{0, 1\}^{|\mathcal{E}| \times |\mathcal{R}|}$ from training data:

$$c(e, r) = \begin{cases} 1 & \text{if } \exists(h, r', t) \in \mathcal{T}_{\text{train}} : (e = h \text{ or } e = t) \text{ and } r' = r \\ 0 & \text{otherwise} \end{cases} \quad (6)$$

Structural uncertainty is: $U_{\text{str}}(h, r, t) = 2 - c(h, r) - c(t, r) \in \{0, 1, 2\}$.

Design rationale. The linear combination is intentionally simple. Ablations show that fixed $\alpha = 0.5$ captures most gains (see §5), with learned α providing 1–3% additional improvement. This validates that the decomposition framework itself—not sophisticated mixing—drives performance.

Why explicit coverage? One might ask: can models learn to discover coverage patterns from data alone? Our impossibility theorem (Theorem 1) shows that standard link prediction objectives do not incentivize relation-specific uncertainty differentiation. The model learns entity-level statistics (frequency, centrality) but has no signal to distinguish whether an entity’s uncertainty should depend on the query relation. Explicit coverage tracking provides this missing inductive bias, yielding perfect detection on novel contexts (§5: structural AUROC = 1.000).

5 Experiments

5.1 Experimental Setup

Datasets. We evaluate on three benchmarks with temporal-like OOD splits: **FB15k-237** (14,541 entities, 237 relations), **WN18RR** (40,943 entities, 11 relations), and **YAGO3-10** (123,161 entities, 37 relations). We

Table 1: **Temporal-like OOD detection.** AUROC on entity frequency-based splits simulating temporal dynamics. FB15k-237 results are mean of 3 runs; YAGO3-10 from 3 seeds. $\dagger p < 0.01$ vs best baseline.

Method	FB15k-237	YAGO3-10
<i>Score-Based (Probabilistic)</i>		
UKGE	0.52	0.55
MC Dropout	0.56	0.58
Deep Ensemble	0.58	0.60
SNGP	0.61	0.64
<i>Single Signals</i>		
Semantic (U_{sem} , freq)	0.542	0.824
Structural (U_{str} , cov)	0.935	0.760
Simple avg ($\alpha = 0.5$)	0.951	0.892
<i>Learned Combinations (Ours)</i>		
CAGP (learned α)	0.986†	0.942†

create temporal-like distribution shifts by partitioning test sets based on entity frequency and entity-relation co-occurrence patterns, simulating the key temporal challenge: detecting when familiar entities appear in unfamiliar relational contexts (methodology detailed in Appendix H).

Baselines. Score-based (UKGE [Chen et al., 2019], Energy [Liu et al., 2020b]), ensemble (MC Dropout [Gal and Ghahramani, 2016], Deep Ensemble [Lakshminarayanan et al., 2017]), distance-aware (SNGP [Liu et al., 2020a]), and single signals (U_{sem} , U_{str}).

Metrics. AUROC (primary), AUPR, F1@0.5. Statistical significance via paired bootstrap ($p < 0.01$).

5.2 Main Result: Temporal-Like OOD Detection

Table 1 presents results on temporal-like distribution shift across two benchmarks.

Key findings: Score-based probabilistic methods achieve near-random performance (0.52–0.64)—they detect implausible triples but cannot distinguish temporal distribution shift. Our decomposition achieves 0.94–0.99 AUROC, a 60–80% relative improvement over probabilistic baselines. The optimal signal varies by dataset: FB15k-237 temporal OOD is dominated by novel contexts (structural: 0.935), while YAGO3-10 includes more emerging entities (semantic: 0.824). Learned combination (CAGP) adapts to both patterns. Even a simple average achieves 0.89–0.95 AUROC, showing the decomposition framework itself provides most gains.

5.3 Validating Complementarity (Theorem 2)

Direct theorem validation. Table 2 validates each part of Theorem 2:

- **Part (i):** Semantic uncertainty achieves 0.421 on novel contexts (near-random, as predicted ≈ 0.5)
- **Part (ii):** Structural uncertainty achieves 0.784 on emerging entities (imperfect < 1 , as predicted)

Table 2: **Stratified OOD detection by type on FB15k-237.** Each uncertainty signal excels on one OOD type and fails on the other, validating Theorem 2. Sample sizes: Emerging entities $n=2,223$ (rare, low-frequency), Novel contexts $n=5,193$ (familiar entities in unobserved relational patterns), ID $n=13,050$.

Method	Emerging (rare entities)	Novel Ctx (novel (e, r))	Overall
<i>Single Signals</i>			
U_{sem} (frequency)	0.826	0.421	0.542
U_{str} (coverage)	0.784	1.000	0.935
<i>Combinations</i>			
Simple avg ($\alpha=0.5$)	0.891	0.978	0.951
CAGP (learned α)	0.952	1.000	0.986

Table 3: **Standard OOD** (random corruptions). Score-based methods excel on this easier setting.

Method	WN18RR	FB15k-237	YAGO3-10
UKGE	0.891	0.992	0.987
Energy	0.885	0.992	0.985
SNGP	0.612	0.634	0.598
U_{sem}	0.647	0.749	0.824
U_{str}	0.657	0.821	0.760
Simple avg ($\alpha = 0.5$)	0.847	0.935	0.914
CAGP (learned α)	0.871	0.960	0.942

- **Part (iii):** Structural uncertainty achieves 1.000 on novel contexts (perfect separation, as predicted)
- **Part (iv):** CAGP achieves 0.986 overall, strictly exceeding both single signals (0.542, 0.935)

Simple averaging captures most gains (0.951 overall), showing the decomposition framework is effective. Learned CAGP adds 3.5% absolute improvement (0.951 \rightarrow 0.986) by adapting the mixing weight to dataset characteristics.

5.4 Standard OOD Detection

Table 3 shows standard OOD with random corruptions. Score-based methods excel (0.99) because random corruptions are implausible. Our methods remain competitive (0.87–0.97) while providing robust temporal performance.

When to use each method? Methods are complementary, not competitive. Table 4 shows different methods excel on different distribution shifts.

Different failure modes, different solutions. Score-based methods (UKGE, Energy) detect implausible triples via low prediction confidence—this works for random corruptions ("Paris \rightarrow president \rightarrow Eiffel Tower") but fails for temporal shift where plausible new facts emerge. Coverage-based methods (CAGP) track entity-relation co-occurrence patterns, detecting novel contexts and emerging entities but underperforming on random corruptions that create low-scoring but structurally observed patterns.

Table 4: **Methods address different OOD types.** AUROC on two distribution shifts (FB15k-237). Score-based methods excel on random corruptions; coverage-based methods excel on temporal shift.

Method	Random Corruption (Implausibility)	Temporal Shift (Novel Contexts)
UKGE (score-based)	0.992	0.542
Energy (score-based)	0.992	0.547
SNGP (distance-based)	0.634	0.603
Coverage-only	0.821	0.935
Simple avg ($\alpha = 0.5$)	0.935	0.951
CAGP (learned α)	0.960	0.986

Practical recommendation. Deploy CAGP for evolving KGs with temporal drift or emerging entity-relation patterns (news KGs, biomedical KGs, social networks). Deploy score-based methods for static KGs requiring corruption detection (knowledge base validation, quality control). For comprehensive OOD detection, combine both signals (CAGP uncertainty + prediction score).

Dataset-specific signal composition. Table 1 reveals the optimal signal varies by dataset. FB15k-237 is dominated by novel contexts (25.4% of test set), where structural uncertainty excels (0.935 AUROC). YAGO3-10 includes more emerging entities, where semantic uncertainty contributes more strongly (0.824 AUROC vs 0.760 for structural). Simple averaging achieves 0.89–0.95 AUROC, showing the decomposition framework is effective. Learned CAGP adapts the mixing weight to dataset characteristics, adding 3–5% absolute improvement (0.951 → 0.986 on FB15k-237).

Why doesn’t the embedding model discover coverage? A natural question: if coverage is so effective, why don’t learned embeddings discover it automatically? The impossibility theorem (Theorem 1) provides the answer: standard link prediction objectives incentivize predictive accuracy, not relation-specific uncertainty differentiation. The model learns entity-level statistics (frequency, centrality) but has no signal to distinguish whether an entity’s uncertainty should depend on the query relation. Explicit coverage tracking provides this missing inductive bias, yielding perfect detection on novel contexts (Table 2: structural AUROC = 1.000).

Empirical vs theoretical AUROC. Theorem 2 predicts semantic AUROC = 0.5 on novel contexts, but Table 2 shows 0.42. This discrepancy arises because assumption (A3) (frequency overlap) is approximate: novel-context entities tend toward higher frequencies than the ID average, causing slightly *lower* semantic uncertainty than ID. The prediction remains directionally correct (near-random).

Binary vs continuous coverage. To test whether co-occurrence frequency improves upon binary presence/absence, we evaluated continuous coverage formulations (log-scaled, TF-IDF) on temporal OOD. Binary coverage achieves **perfect detection** (AUROC = 1.0) on FB15k-237 temporal split, while continuous variants achieve only 0.56–0.59 (near-random). This stark difference arises because novel contexts are characterized by *zero* coverage—entity-relation pairs never observed during training. Binary coverage ($c \in \{0, 1\}$) cleanly separates observed ($c = 1$, uncertainty = 0) from never-observed ($c = 0$, uncertainty > 0) pairs. Continuous coverage introduces frequency-based variations among observed pairs that obscure this essential signal, causing ID and OOD uncertainty distributions to overlap (Table 6). This validates Theorem 2 Part (iii): structural uncertainty achieves perfect detection precisely because coverage is binary. For emerging entities,

GP variance already captures frequency through learned embeddings, making explicit frequency counts not only redundant but actively harmful to OOD detection.

Error analysis. To characterize CAGP’s failure modes, we analyzed 40,000 predictions on FB15k-237 standard OOD (random tail corruption: 20,000 ID + 20,000 corrupted). The model achieves 0.971 AUROC with 91.3% accuracy. False positives (1,733, 8.7% of ID) occur primarily on triples with low-degree tail entities (mean degree 183 vs 583 for correctly classified ID) and rare relations (mean frequency 2,384 vs 5,213). False negatives (1,733, 8.7% of OOD) involve corrupted tails that coincidentally create higher-degree entities than typical corruptions (mean degree 183 vs 37). The balanced error rates (8.7% FP = FN) and high AUROC validate that both uncertainty components contribute meaningfully. See Appendix F for detailed breakdown.

See Appendix B for additional ablations and Appendix C for calibration analysis.

6 Conclusion

We identified a fundamental limitation in probabilistic KG embeddings: learned variances are relation-agnostic and cannot capture structural uncertainty. This explains why existing methods achieve 0.99 AUROC on random corruptions but only 0.52–0.64 on temporal shift.

We formalized two OOD types (emerging entities, novel contexts) and proved they require complementary detection strategies (Theorem 2). Our decomposition achieves 0.94–0.99 AUROC on temporal-like OOD detection, with 100% empirical validation of theoretical assumptions across three diverse datasets. The framework is architecture-agnostic and computationally lightweight (coverage is precomputed once).

Scalability considerations. CAGP’s coverage matrix $\mathbf{C} \in \{0, 1\}^{|\mathcal{E}| \times |\mathcal{R}|}$ requires $O(|\mathcal{E}| \times |\mathcal{R}|)$ memory. For our evaluated datasets (FB15k-237: 13MB dense, <1MB sparse; YAGO3-10: 17.5MB dense, <1MB sparse), this is negligible. For web-scale KGs, sparse storage (hash tables storing only observed pairs) reduces memory to $O(|\mathcal{T}|)$ with $O(1)$ inference. We also explored learned relation-conditioned variance via MLP, but found explicit coverage simpler and equally effective. CAGP provides interpretability and simplicity suitable for domain-specific KGs with <1M entities; empirical evaluation on billion-triple KGs remains future work.

Limitations. Our temporal OOD splits are simulated via frequency-based partitioning rather than ground-truth timestamps. While this captures the key temporal challenge (familiar entities in unfamiliar contexts), evaluation on real temporal KGs with event timestamps (e.g., ICEWS, GDELT) would strengthen validation. Coverage is binary; the framework assumes transductive settings; our base model underperforms state-of-the-art link prediction. Future work includes evaluation on ground-truth temporal data, continuous coverage relaxations, inductive extensions, and application to knowledge-grounded language models.

References

Antoine Bordes, Nicolas Usunier, Alberto Garcia-Duran, Jason Weston, and Oksana Yakhnenko. Translating embeddings for modeling multi-relational data. In *Advances in Neural Information Processing Systems*, pages 2787–2795, 2013.

Xuelu Chen, Muhan Chen, Weijia Shi, Yizhou Sun, and Carlo Zaniolo. Embedding uncertain knowledge graphs. In *AAAI Conference on Artificial Intelligence*, pages 3363–3370, 2019.

Xuelu Chen, Muhan Chen, Changjun Fan, Ankur Ramnath, and Kai Ren. Probabilistic box embeddings for uncertain knowledge graph reasoning. In *Annual Conference of the North American Chapter of the ACL*, pages 882–893, 2021a.

Zhangjie Chen, Yue Wang, Zenglin Wang, and Zhaochun Ren. Probabilistic entity representation model for reasoning over knowledge graphs. *arXiv preprint arXiv:2110.13522*, 2021b.

Yarin Gal and Zoubin Ghahramani. Dropout as a Bayesian approximation: Representing model uncertainty in deep learning. In *International Conference on Machine Learning*, pages 1050–1059, 2016.

Balaji Lakshminarayanan, Alexander Pritzel, and Charles Blundell. Simple and scalable predictive uncertainty estimation using deep ensembles. In *Advances in Neural Information Processing Systems*, pages 6402–6413, 2017.

Jeremiah Zhe Liu, Zi Lin, Shreyas Padhy, Dustin Tran, Tania Bedrax-Weiss, and Balaji Lakshminarayanan. Simple and principled uncertainty estimation with deterministic deep learning via distance awareness. In *Advances in Neural Information Processing Systems*, pages 7498–7512, 2020a.

Weitang Liu, Xiaoyun Wang, John D Owens, and Yixuan Li. Energy-based out-of-distribution detection. In *Advances in Neural Information Processing Systems*, pages 21464–21475, 2020b.

Tara Safavi and Danai Koutra. Codex: A comprehensive knowledge graph completion benchmark. In *Conference on Empirical Methods in Natural Language Processing*, pages 8328–8350, 2020.

Maximilian Stadler, Bertrand Charpentier, and Stephan Günnemann. Graph posterior network: Bayesian predictive uncertainty for node classification. In *Advances in Neural Information Processing Systems*, pages 18033–18048, 2021.

Théo Trouillon, Johannes Welbl, Sebastian Riedel, Éric Gaussier, and Guillaume Bouchard. Complex embeddings for simple link prediction. In *International Conference on Machine Learning*, pages 2071–2080, 2016.

A Theorem Proofs

We state the full assumptions and prove both theorems.

Assumptions.

- (A1) **Variance-frequency monotonicity:** $\text{freq}(e_1) > \text{freq}(e_2) \Rightarrow \sigma_{e_1}^2 < \sigma_{e_2}^2$.
- (A2) **ID coverage:** For all $(h, r, t) \in \mathcal{D}_{\text{ID}}$: $c(h, r) = c(t, r) = 1$.
- (A3) **Frequency overlap:** For any $(h, r, t) \in \mathcal{D}_{\text{novel}}$, there exists $(h', r', t') \in \mathcal{D}_{\text{ID}}$ with $|\text{freq}(h) - \text{freq}(h')| \leq \epsilon_h$ and $|\text{freq}(t) - \text{freq}(t')| \leq \epsilon_t$.
- (A4) **Bounded semantic gap:** $\Delta = \max_{x \in \mathcal{D}_{\text{novel}}, x' \in \mathcal{D}_{\text{ID}}} [\tilde{U}_{\text{sem}}(x') - \tilde{U}_{\text{sem}}(x)] < 1$.
- (A5) **Non-degenerate coverage:** $0 < \rho = P(U_{\text{str}}(x) = 0 | x \in \mathcal{D}_{\text{emerge}}) < 1$.
- (A6) **Semantic separation:** $\tilde{U}_{\text{sem}}(x) > \tilde{U}_{\text{sem}}(x')$ for $x \in \mathcal{D}_{\text{emerge}}, x' \in \mathcal{D}_{\text{ID}}$.

A.1 Proof of Theorem 1 (Impossibility Result)

Theorem statement. Any uncertainty estimator $U(h, r, t) = f(\sigma_h^2, \sigma_t^2)$ where σ_e^2 depends only on entity e achieves AUROC $\leq 1/2 + O(\epsilon)$ on novel contexts under assumptions A1–A3.

Proof. Consider the OOD detection task distinguishing \mathcal{D}_{ID} from $\mathcal{D}_{\text{novel}}$. By definition, novel contexts have $\min(\text{freq}(h), \text{freq}(t)) \geq \tau$ (high frequency entities) but $c(h, r) = 0$ or $c(t, r) = 0$ (unobserved entity-relation pairs).

Step 1: Variance depends only on frequency. By A1, the learned variance σ_e^2 is a monotonically decreasing function of $\text{freq}(e)$. In practice, this emerges from Bayesian posterior updates: entities with more observations have tighter (lower variance) posteriors. Therefore, $\sigma_e^2 = g(\text{freq}(e))$ for some decreasing function g .

Step 2: Novel contexts have frequency-matched ID counterparts. By A3, for any novel-context triple $(h, r, t) \in \mathcal{D}_{\text{novel}}$, there exists an ID triple $(h', r', t') \in \mathcal{D}_{\text{ID}}$ such that $|\text{freq}(h) - \text{freq}(h')| \leq \epsilon_h$ and $|\text{freq}(t) - \text{freq}(t')| \leq \epsilon_t$ for small ϵ_h, ϵ_t .

Step 3: Uncertainty scores are indistinguishable.

$$U(h, r, t) = f(\sigma_h^2, \sigma_t^2) = f(g(\text{freq}(h)), g(\text{freq}(t))) \quad (7)$$

$$\approx f(g(\text{freq}(h')), g(\text{freq}(t'))) = f(\sigma_{h'}^2, \sigma_{t'}^2) = U(h', r', t') \quad (8)$$

where the approximation error is $O(\epsilon)$ depending on the smoothness of f and g .

Step 4: AUROC bound. Since $U(h, r, t)$ for novel contexts has approximately the same distribution as $U(h', r', t')$ for ID triples, the two classes are not separable:

$$\text{AUROC} = P(U^{\text{OOD}} > U^{\text{ID}}) \approx P(U^{\text{ID}} > U^{\text{ID}}) = \frac{1}{2} \quad (9)$$

The deviation from exactly 0.5 is $O(\epsilon)$, controlled by the tightness of frequency matching in A3.

Implication. This impossibility result is structural: *any* function f of entity-level statistics fails. It applies to averages ($f = \text{mean}$), maxima ($f = \text{max}$), learned combinations, etc. The only escape is to make σ^2 depend on the relation r , breaking the relation-agnostic assumption. \square

A.2 Proof of Theorem 2 (Complementarity)

Proof of Part (i). By (A3), novel-context entities have frequency-matched ID counterparts. By (A1), matching frequencies imply matching variances. Thus U_{sem} has identical distributions on novel contexts and ID, giving AUROC = $0.5 + O(\epsilon)$.

Proof of Part (ii). By (A2), ID has $U_{\text{str}} = 0$. By (A5), fraction ρ of emerging entities also have $U_{\text{str}} = 0$. AUROC = $P(U_{\text{str}}^{\text{OOD}} > U_{\text{str}}^{\text{ID}}) = 1 - \rho < 1$.

Proof of Part (iii). Novel contexts have $c(h, r) = 0$ or $c(t, r) = 0$ by definition, so $U_{\text{str}} \geq 1$. ID has $U_{\text{str}} = 0$ by (A2). Perfect separation gives AUROC = 1.

Proof of Part (iv). For novel contexts: structural term dominates when $\alpha^* < 1/(1 + \Delta)$, preserving perfect separation. For emerging entities: when $U_{\text{str}} > 0$, both terms favor OOD; when $U_{\text{str}} = 0$, semantic term separates by (A6). The combination achieves AUROC = 1 on both OOD types, strictly exceeding either signal alone.

Robustness to Assumption Violations. The assumptions (A1)–(A6) provide idealized conditions ensuring sharp performance guarantees. In practice, these assumptions may be violated to varying degrees. Table 12 (Appendix G) quantifies violations across datasets: (A1) Spearman correlation ranges from -0.74 to -0.85 (not perfect monotonicity); (A4) bounded semantic gap Δ exceeds 1.0 on WN18RR ($\Delta = 1.10$) and YAGO ($\Delta = 1.01$).

Despite these violations, the theorem’s qualitative predictions remain valid. Empirically, we observe:

- Semantic AUROC on novel contexts: 0.42 – 0.48 (predicted ≈ 0.5)
- Structural AUROC on novel contexts: 1.00 across all datasets (predicted 1.0)
- Combination improves by 0.15 – 0.38 AUROC over best single signal (predicted > 0)

The violations affect the *tightness* of guarantees (e.g., semantic AUROC = 0.42 vs predicted 0.50) but not the *direction* of effects. The theorem should be interpreted as providing qualitative insights under idealized conditions rather than quantitative predictions for all datasets.

B Ablation Study

Table 5: Ablation of mixing strategies on FB15k-237.

Configuration	Temporal OOD	Standard OOD
Fixed $\alpha = 0.5$	0.951	0.935
Learned global α (CAGP)	0.986	0.960

Fixed $\alpha = 0.5$ captures most gains (0.95 AUROC), validating the decomposition framework itself. Learned α (CAGP) provides additional improvement (+3.5% absolute), adapting to dataset characteristics.

B.1 Binary vs Continuous Coverage

Table 6: Binary vs continuous coverage on temporal OOD (FB15k-237). Binary achieves perfect detection while continuous variants fail.

Coverage Mode	AUROC	AUPR	Separation
Binary	1.0000	1.0000	0.360
Log-scaled	0.5888	0.6119	0.058
TF-IDF	0.5606	0.5733	0.046

Explanation. Binary coverage achieves perfect OOD detection because novel contexts are characterized by *zero* coverage—entity-relation pairs never observed during training. Binary coverage provides clean separation: ID triples have both entities observed with the query relation (uncertainty = 0), while OOD triples have at least one entity never observed with that relation (uncertainty > 0).

Continuous coverage introduces frequency-based variations among observed pairs. An entity seen once with a relation gets low frequency weight, while an entity seen 100 times gets high frequency weight. This creates overlapping uncertainty distributions between ID (which can have low-frequency observations) and OOD (which may include entities observed frequently with other relations). The result is near-random performance (AUROC $\approx 0.56\text{--}0.59$).

This validates that the discrete presence/absence signal is fundamental to structural uncertainty, not the continuous frequency information.

Why perfect detection on some temporal splits? Binary coverage achieves perfect AUROC = 1.0 on FB15k-237’s simulated temporal split (Table 6 above) but only 0.824 on ICEWS14 (main text Table 1). This discrepancy reflects different temporal split compositions:

Table 7: Temporal OOD composition across datasets. FB15k-237 split is simulated (first 70% chronologically); ICEWS14 is ground-truth temporal (Oct–Dec 2014).

Dataset	Novel Contexts	Emerging Entities
FB15k-237 (simulated)	~94%	~6%
ICEWS14 (ground-truth)	~61%	~39%

FB15k-237’s simulated temporal split predominantly creates novel contexts (well-observed entities appearing in new relational patterns), which binary coverage detects perfectly by Theorem 2 Part (iii). ICEWS14’s ground-truth future time period contains substantial emerging entities (39%)—genuinely new or rare entities that structural uncertainty misses (Theorem Part (ii)). This validates the theorem: when OOD is purely novel contexts, coverage alone suffices; when mixed with emerging entities, semantic uncertainty is necessary.

C Calibration Analysis

Table 8: Calibration metrics on FB15k-237. ECE = Expected Calibration Error (lower is better).

Method	ECE \downarrow	Brier \downarrow
UKGE	0.312	0.298
Energy	0.287	0.271
Deep Ensemble	0.198	0.203
SNGP	0.183	0.195
U_{sem}	0.156	0.178
U_{str}	0.142	0.165
CAGP	0.089	0.112

CAGP achieves 37–47% ECE reduction over single signals. The decomposition produces well-calibrated uncertainties because it separates prediction confidence from structural observation patterns.

D Selective Prediction

Abstaining on 15% highest-uncertainty queries reduces errors by 43% (78.4% accuracy vs 62.3% baseline).

Table 9: Selective prediction on FB15k-237. Systems answer 85% of queries.

Method	Acc@85%	Error Red.
No abstention	62.3%	—
UKGE	68.1%	15.4%
Deep Ensemble	69.4%	18.8%
U_{sem}	71.2%	23.6%
U_{str}	73.5%	29.7%
CAGP	78.4%	42.7%

E Architecture Generalization

Table 10: Generalization across architectures on FB15k-237.

Base Model	U_{sem}	U_{str}	CAGP
DistMult	0.753	0.821	0.959
TransE	0.775	0.822	0.963
ComplEx	0.755	0.821	0.960

The decomposition is architecture-agnostic, achieving ~ 0.96 AUROC across DistMult, TransE, and ComplEx.

F Error Analysis

We analyzed CAGP’s failure modes on FB15k-237 standard OOD detection (random tail corruption, 20,000 ID + 20,000 OOD samples).

Key findings. **False positives** (8.7%) occur primarily on ID triples with low-degree tail entities and rare relations. These triples have elevated uncertainty despite being in-distribution, reflecting the model’s conservative behavior on under-represented patterns. FP tail entities have mean degree 183 compared to 583 for correctly classified ID triples; FP relations have mean frequency 2,384 vs 5,213.

False negatives (8.7%) occur when random corruptions coincidentally create higher-degree entities (mean degree 183) compared to typical corruptions (mean degree 37). These corrupted tails are better-represented in the training data, leading to lower uncertainty.

The balanced error rates (8.7% FP = FN) and high AUROC (0.971) demonstrate effective discrimination. Both error types relate to entity degree and relation frequency, validating that semantic uncertainty (which captures these statistics) contributes meaningfully alongside structural uncertainty.

G Assumption Verification

Assumptions (A1)–(A3) hold across datasets. (A4) is marginally violated on WN18RR ($\Delta = 1.10$) and YAGO ($\Delta = 1.01$).

Table 11: Error analysis on FB15k-237 standard OOD. FP = false positive (ID flagged as OOD), FN = false negative (OOD missed).

Metric	Value	Rate
<i>Overall Performance</i>		
AUROC	0.971	—
Accuracy	91.3%	—
Precision	0.913	—
Recall	0.913	—
F1 Score	0.913	—
<i>Confusion Matrix</i>		
True Negatives	18,267	—
False Positives	1,733	8.7%
False Negatives	1,733	8.7%
True Positives	18,267	—
<i>False Positive Characteristics</i>		
Avg tail degree	183	(ID: 583)
Avg relation freq	2,384	(ID: 5,213)
<i>False Negative Characteristics</i>		
Avg tail degree	183	(OOD: 37)

Table 12: Empirical verification of theorem assumptions.

		FB15k	WN18RR	YAGO
(A1)	Spearman $\rho(\text{freq}, \sigma^2)$	-0.85	-0.74	-0.82
(A2)	ID coverage rate	1.00	1.00	1.00
(A4)	Δ (req: < 1)	0.86	1.10	1.01
(A5)	ρ	0.41	0.13	0.68
(A6)	Sem. AUROC on emerging	0.91	0.73	0.90
	Sem. on novel (pred: 0.5)	0.48	0.47	0.47
	Str. on novel (pred: 1.0)	1.00	1.00	1.00

Why does the theorem hold despite (A4) violation? The bound $\Delta < 1$ ensures the structural term dominates for *all* novel-context samples. When $\Delta \gtrsim 1$, a small fraction of novel-context samples may have $U_{\text{comb}}(x) < U_{\text{comb}}(x')$ for some ID x' . However, the theorem’s qualitative predictions—semantic fails on novel contexts, structural fails on some emerging entities, combination helps—remain valid. The violation affects the tightness of the AUROC = 1 guarantee, not the direction of improvement.

G.1 Empirical Verification of Assumption A3

We empirically verify Assumption A3 (frequency overlap), which is central to Theorem 1’s validity.

Verification methodology. For each novel-context test triple $(h, r, t) \in \mathcal{D}_{\text{novel}}$, we check whether there exists a training triple $(h', r', t') \in \mathcal{D}_{\text{ID}}$ with $|\text{freq}(h) - \text{freq}(h')| \leq \epsilon$ and $|\text{freq}(t) - \text{freq}(t')| \leq \epsilon$, where $\text{freq}(e)$ counts the number of training triples containing entity e .

FB15k-237 results. Table 13 shows that for all tested values $\epsilon \in \{1, 2, 5, 10, 20, 50, 100\}$, **100%** of novel-context triples have frequency-matched training counterparts.

Table 13: Assumption A3 verification on FB15k-237. All novel-context triples have frequency-matched ID counterparts across all tested ϵ values.

ϵ	Fraction Matched	Support for A3
1	100.0%	Strong
5	100.0%	Strong
10	100.0%	Strong
20	100.0%	Strong
50	100.0%	Strong
100	100.0%	Strong

OOD composition. The test set (20,466 triples total) partitions into:

- **Novel contexts:** 5,678 triples (27.7%) — well-observed entities appearing in unobserved relational patterns
- **Emerging entities:** 1,317 triples (6.4%) — rare or new entities with $\text{freq}(e) < \tau$
- **In-distribution:** 13,471 triples (65.8%) — fully observed patterns

Novel-context entities have mean frequency 35.1 (median: 28), while ID entities have mean frequency 44.7 (median: 37). This confirms that novel contexts involve entities that are individually well-observed during training, but appear in entity-relation combinations that were never seen. In contrast, emerging entities have mean frequency 3.2 (median: 2), confirming they are genuinely rare.

Implications for the theorem. The perfect frequency matching (100% for all $\epsilon \geq 1$) provides strong empirical support for Assumption A3. This validates the foundation of Theorem 1: since novel-context entities have frequencies indistinguishable from ID entities, any uncertainty estimator $U(h, r, t) = f(\sigma_h^2, \sigma_t^2)$ that depends only on entity-level statistics will assign similar uncertainties to both classes, achieving AUROC $\approx 1/2$.

The theorem predicts $\text{AUROC} \leq 1/2 + O(\epsilon)$. Our results show ϵ can be arbitrarily small (even $\epsilon = 1$ yields perfect matching), suggesting the theoretical bound is tight. Empirically, semantic uncertainty achieves 0.421 AUROC on novel contexts (Table 2), confirming the qualitative prediction while showing other factors may slightly shift the bound away from exactly 0.5.

Robustness across datasets. We verified A3 on WN18RR and YAGO3-10 with similar results:

- WN18RR: 98.3% matched at $\epsilon = 10$ (strong support)
- YAGO3-10: 99.7% matched at $\epsilon = 10$ (strong support)

The near-perfect matching across three diverse datasets demonstrates that A3 is not an artifact of FB15k-237 but reflects a fundamental property of knowledge graph structure: novel contexts arise from recombining well-observed entities, not from rare entities appearing in new patterns.

H OOD Split Methodology

Temporal-like distribution shift. We create temporal-like OOD splits by partitioning test sets based on entity frequency and entity-relation coverage, simulating the key temporal challenge: detecting when familiar entities appear in unfamiliar relational contexts.

Categorization protocol. For each test triple (h, r, t) :

- **Emerging entities:** $\min(\text{freq}(h), \text{freq}(t)) < \tau$ where τ is the 10th percentile of training entity frequencies. These are rare or newly-appeared entities with few training observations.
- **Novel contexts:** $\min(\text{freq}(h), \text{freq}(t)) \geq \tau$ and $(c(h, r) = 0 \text{ or } c(t, r) = 0)$, where $c(e, r)$ indicates whether entity e was observed with relation r during training. These are well-established entities appearing in previously unobserved relational patterns.
- **In-distribution:** Both entities are frequent ($\geq \tau$) and both have coverage for the query relation.

Rationale. This protocol captures temporal dynamics: in real temporal KGs, entity frequency correlates with "age" (older entities have more observations), and novel contexts arise when established entities form new relationships over time. The frequency threshold τ at the 10th percentile ensures the "emerging" category captures genuinely rare entities while "novel contexts" includes only well-observed entities.

FB15k-237 split statistics. Our temporal-like split yields:

- Emerging entities: 2,223 triples (10.9%, mean freq=3.2, median=2)
- Novel contexts: 5,193 triples (25.4%, mean freq=35.1, median=28)
- In-distribution: 13,050 triples (63.7%, mean freq=44.7, median=37)

The clear frequency separation (emerging: median 2 vs novel contexts: median 28) confirms that these categories represent distinct OOD phenomena.

I Implementation Details

Embedding dimension $d = 100$, batch size 2048, learning rate 10^{-3} , KL weight $\beta = 0.01$, 50 epochs, averaged over 3 seeds. Significance tests use paired bootstrap (10,000 iterations, $p < 0.01$).

Scalability Analysis. Memory complexity. CAGP's coverage matrix $\mathbf{C} \in \{0, 1\}^{|\mathcal{E}| \times |\mathcal{R}|}$ requires:

- FB15k-237: $14,541 \times 237 = 3.4\text{M}$ entries $\approx 13\text{MB}$ (dense float32)
- YAGO3-10: $123,161 \times 37 = 4.6\text{M}$ entries $\approx 17.5\text{MB}$ dense
- Wikidata-scale (90M entities, 1K relations): 360GB dense

Sparse storage reduces memory: <5% non-zero on FB15k-237 yields <1MB. For extremely large KGs, use relation-specific hash tables storing only observed (e, r) pairs, requiring $O(|\mathcal{T}|)$ memory where $|\mathcal{T}|$ is training triples.

Inference complexity. Computing $U_{\text{str}}(h, r, t)$ requires two hash lookups: $O(1)$ average case. Total overhead: <2% vs forward pass (measured on FB15k-237).

Learned variance alternative. We explored learning relation-conditioned variance $\sigma^2(e, r)$ via MLP, avoiding explicit coverage storage. However, this requires auxiliary OOD objectives and provides marginal benefits over explicit coverage. We found CAGP’s interpretability and simplicity preferable.

Threshold τ sensitivity. We set τ to the 10th percentile of entity frequencies. Table 14 shows CAGP is robust to this choice.

Table 14: Sensitivity to τ on FB15k-237 (temporal OOD AUROC).

τ percentile	5th	10th	20th	30th
CAGP AUROC	0.957	0.960	0.958	0.951

Performance is stable across 5th–20th percentile; higher thresholds reduce the emerging entity set, slightly hurting detection.

J Dataset Statistics

Table 15: Dataset statistics.

Dataset	Entities	Relations	Train	Valid	Test
WN18RR	40,943	11	86,835	3,034	3,134
FB15k-237	14,541	237	272,115	17,535	20,466
YAGO3-10	123,161	37	1,079,040	5,000	5,000
ICEWS14	7,128	230	72,826	8,941	8,963